 doi:10.20944/preprints202102.0610.v1

Article

Analysis of Default Mode Network in Social Anxiety Disorder: EEG Resting-State Effective Connectivity Study

Abdulhakim Al-Ezzi [1]*, Nidal Kamel[1], Ibrahima Faye [1], and Esther Gunaseli [2]

[1] Centre for Intelligent Signal and Imaging Research (CISIR) Department of Electrical and Electronic Engineering, Universiti Teknologi PETRONAS, Malaysia
[2] Universiti Kuala Lumpur, Psychiatry Discipline Sub Unit, Perak, Malaysia
* Correspondence: abduhalezzy@yahoo.com

Abstract: Several neuroimaging findings by using different modalities (e.g., fMRI and PET) have suggested that social anxiety disorder (SAD) is correlated with alterations in regional or network-level brain function. However, these modalities do not quantify the fast dynamic connectivity of causal information networks due to their poor temporal resolution. In this study, SAD-related changes in brain connections within the default mode network (DMN) was investigated using Electroencephalogram (EEG). Partial directed coherence (PDC) was used to assess the causal influences of DMN regions on each other and indicate the changes in the DMN effective network related to SAD severity. The EEG data were collected from 88 subjects (control, mild, moderate, severe) and used to estimate the effective connectivity between DMN regions at different frequency bands. Among the healthy control (HC) and the three considered levels of severity of SAD, the results indicated a higher level of causal interactions for the mild and moderate SAD groups than for the severe and HC groups. Between the control and the severe SAD groups, the results indicated a higher level of causal connections for the control throughout all the DMN regions. We found significant increases in the mean PDC in the delta and alpha bands between the SAD groups. Among the DMN regions, the precuneus exhibited a higher level of causal influence than other regions. Therefore, it was suggested to be a major source hub that contributes to the mental exploration and emotional content of SAD. In contrast to the severe group, the HC exhibited higher resting-state connectivity at the mesial prefrontal cortex (mPFC), providing evidence for mPFC dysfunction in the severe SAD group. Furthermore, the total Social Interaction Anxiety Scale (SIAS) was positively correlated with the mean values of the PDC of the severe SAD group and negatively correlated with those of the HC group. The reported results may facilitate greater comprehension of the underlying potential SAD neural biomarkers and can be used to characterize possible targets for further medication.

Keywords: Effective connectivity network, Partial directed coherence (PDC), Social Anxiety Disorder (SAD), Default Mode Network (DMN), Electrophysiological biomarkers (EEG), Resting state network (RSN), Granger causality (GC).

1. Introduction

Social anxiety disorder (SAD) is a prevalent psychiatric health condition identified by persistent panic and avoidance in a domain of social tasks that involve a possibility of scrutiny by others [1]. Cognitive models underline the discriminatory processing of interior and exterior threat signals that SAD individuals engage in when confronted with others (e.g., negative beliefs, attentional prejudice to disinclination faces [2] as an indicator of the expansion and preservation of the SAD [3], [4]. Accumulating evidence from experiment-based functional magnetic resonance imaging (fMRI) studies in recent years, including aversive biomarkers, revealed such biases in the findings of fronto-limbic disruptions,

 doi:10.20944/preprints202102.0610.v1

resulting in limbic/paralimbic neural alterations in the emotional processing system (e.g., hippocampus, amygdala, and insula) and deviant activity (greater or smaller activations) in the neuronal areas that controlled emotional responses (e.g., anterior cingulate cortex (ACC), dorsolateral prefrontal cortex; dPFC) [5] and altered activity in the prefrontal cortex [6].Moreover, the right insula have positive causal effects on the dPFC, which would provide a significant and new platform for investigating the pathological anomalies in SAD [7], [8]. A previous systematic review of SAD indicated that adolescents and children with SAD exhibit emotional dysregulation in different domains of the emotion regulation system, such as enhanced social avoidance, more safety behaviors, recurrent negative thinking, biased perception and awareness of social information, and deficiencies in emotional expression [9].

The SAD's neurobiological effects have been confirmed by baseline resting-state fMRI studies, which allow substantial (instantaneous, task-independent) neural networks to be examined. Studies have revealed aberrant interactions in the SAD within spatially distant regions, indicating that the dysfunction includes a disturbance of the baseline in decentralized neural systems. For example, a reduced frontal limbic functional connectivity (FC) and aberrant effective connectivity (EC) were observed in SAD groups compared with HC groups [10], [11]. Additionally, in SAD patients, significant variations in task-positive and task-negative networks (e.g., attention network, DMN, visual networking system) were observed [12]. Overall, the fMRI results suggest abnormal resting-state behaviors, and these behaviors can reflect a threat-sensitive network in SAD. However, the current findings of neural networks in the brain that are linked to essential activation are restricted in fMRI owing to its low temporal resolution. Thus, fMRI does not detect the millisecond to second timescales, (short timescales represent significant information processing at rest).

Another more effective neuroimaging approach is EEG, which evaluates the rapid and lagged instantaneous brain activation in both time and frequency scales, so that actual neurobehavioral networks can be identified [13]. While various concepts of positive and negative impacts in SAD have been posited, mainly on the basis of self-reported questionnaires, interpersonal interactions, and behavioral analyses [14], less is understood about how SAD is being interpreted at the neural level. One approach for addressing this problem is to investigate how neural brain activity in SAD communicates using EEG throughout DMN processing. To date, EEG has hardly been applied in research on the EC of SAD at rest. In several studies, the EEG method was employed to investigate SAD's cognitive models and behavioral mechanisms in social engagement tasks, visual tasks, and DMN, for review [15] . SAD patients have exhibited reduced connectivity in the right mPFC and right inferior parietal gyrus compared with HCs, indicating that SAD is associated with attention deficiency an impairment in cognitive function in SAD [16].

Among the resting-state elements, the DMN received great attention nowadays [17], [18]. The DMN is localized in three regions; precuneus/posterior cingulate cortex (PCC), (LPC), and mPFC. Science suggests that the DMN is capable to contribute to the psychological exploration of emotional and social functionality, which can help to study the neural symptoms of SAD. The DMN is perceived to be partially responsible for the intestinal consciousness. It covers the posterior and anterior cortical midline structures, with major hubs located in the PCC, precuneus, mPFC, and angular gyrus [17]. The DMN has exhibited higher activation in the resting state when a person becomes more concentrated internally rather than externally or on attention-demanding tasks [19]. SAD individuals have exhibited significant enhancements in the interconnections in the cortical brain, mainly in the precuneus, which is an essential component of the DMN [20]. Additionally, SAD patients exhibited significant correlations with the substantial regions involved in precuneus, PCC, and parietal sites in the DMN during the expectation, emotional excitement, awareness regulation, and reception of monetary gain [21],[22]. In the salience network, SAD individuals exhibited an enhanced FC within the left precuneus and left supramarginal gyrus in the DMN, compared with the HC group [23], [24]. Thus, it seems

Preprints (www.preprints.org) | NOT PEER-REVIEWED | Posted: 26 February 2021 doi:10.20944/preprints202102.0610.v1

reasonable that precuneus activity influences the neurocorrelates of cortical and subcortical connections involved in the production of highly sophisticated information processing rather than direct external stimuli processing [25]. Neurobiological models of SAD suggest that disturbances in the elaboration of the amygdala-prefrontal network and hippocampus are stronger in SAD individuals [7], [26].

The main objective of our study is to estimate the severity of SAD by categorizing its grades (severe, moderate, mild, and HC) using EC (PDC algorithm). Connectivity evidences can be derived from dynamic causal modeling in the EC technique, which calculates and assesses the negative or positive influences of one location on another and reveals how these influences are impacted by the stimuli type and the design of the experiment. Nonetheless, a clear understanding of neuronal pathways is likely to demand the discovery of directed FC (effective connectivity). The Granger causality (GC) is an efficient technique for extracting this connectivity from the neuronal information [27]. The GC and other relevant concepts, in contrast to the bi-directional FC, which is a model-free construct, quantifies the unidirectional EC and examines asymmetrical cause's correlations within the neural networks. Two alternate tests directly related to spectral the GC are the partial directed coherence (PDC) [28] and the directed transfer function (DTF) [29]. A review of techniques for evaluating the directed connectivity using data from multiple channels was published [30].

To the best of our knowledge, this was the first DMN analysis in which the severity of SAD (severe, average, mild, and control) was evaluated by using the effective connectivity measures (PDC) to assess effective network characteristics at different frequencies (delta, theta, alpha, low beta, and high beta). Our initial research concern was whether SAD is correlated with disrupted neural activation in DMN processing. It was hypothesized that the four SAD groups would respond differently in the DMN resting state, stimulating brain interactions between various brain regions and enhancing the EC of the brain cognitive network. The spectral EC was used to characterize the directions, power intensity, and influences

The following are presented in the remainder of this paper: materials and methods (for data acquisition), statistical dimensions, results (scientific findings), discussions, limitations, and potential directions with conclusions.

2. Materials and Methods

2.1. Participants

Eighty-nine (89) participants were chosen from 417 respondents (34 females and 54 males; 17–25 years old (mean (M) = 22.35, standard deviation (SD) = 0.98) (M = 23.16, SD = 0.85)) who submitted SIAS self-assessment reports [31]. The adequate sample size was defined by performing a power analysis in G*Power [32]. Respondents of both genders were enrolled in the experiment to generalize the study's findings and validate the findings of our study. Table 1 shows the demographics data and group characteristics. Depending on the SIAS scores, the participants were divided into four categories: the control group (SIAS score < 20), mild group (SIAS score < 35), average group (SIAS score < 50), and severe group (SIAS score ≥ 50). The selected participants have been diagnosed with SAD using the DSM-IV-based Composite International Diagnostic Interview [33]. One (1) participant was excluded because of data-collection issues. The groups did not differ significantly with regard to age: $F(1, 87) = 2.664$, $p = 054$, $\eta 2 = 0.093$. None of the subjects had a history of psychological, neurological, or surgical deficiency that may have affected their brain activity or metabolic processes. At the time of recruitment and during the EEG session, no subjects had received any pharmacological or psycho-therapeutic treatment. All the recruited subjects were given a single sheet containing both information about the research and a waiver of written informed consent, and they were compensated for their time and cooperation. The experiment complied with the Helsinki Declaration [34]. The protocol for the study was carefully reviewed, accepted, and approved by the Medical

Preprints (www.preprints.org) | NOT PEER-REVIEWED | Posted: 26 February 2021 doi:10.20944/preprints202102.0610.v1

Research Ethics Committee of the Royal College of Medicine Perak, Kuala Lumpur University with code number (UniKLRCMP/MREC/2019/065) on 17 September 2019.

Table 1. Demographic data and group characteristics

Group	Number of participants		Total	Age		SIAS score	
	Female	Male		Female	Male	Female	Male
Severe	12	10	22	22.13 ± 2.78	23.11 ± 1.02	67.53 ± 6.21	66.81 ± 5.32
Moderate	7	15	22	21.98 ± 3.11	22.21 ± 1.25	55.7 3± 7.81	54.41 ± 6.61
Mild	12	10	22	22.61 ± 2.32	21.71 ±2 .31	38.32 ± 512	37.71 ± 5.81
Control	8	14	22	21.76 ± 1.73	23.62 ± 1.65	14.71 ± 6.74	16.61 ± 7.34

2.2. Experimental Design

The rest-state recordings were conducted in an EEG laboratory. The participants were asked to sit comfortably, keeping their eyes closed, in a comfortable, semi-darkened dim room. The subjects were requested to abstain from consuming alcohol and caffeine prior to their EEG recording (for at least 5 h). The subjects were instructed to habituate themselves to the procedure of the EEG recording task prior to the experiment. The participants then were provided with a description of the EEG protocol and signed an informed consent form. After the electrodes were mounted on the scalp, the EEG protocol was started to acquire the resting state of the EEG for 5 min (eyes closed). The participants were informed to close their eyes, remain calm, and let their minds wander freely. Eventually, all the participants answered the self-report questionnaires and were debriefed.

2.3. EEG data acquisition, preprocessing and PDC implementation

Scalp EEG signals were continuously acquired during a 5-min baseline (3 second-eyes closed) duration using a referential 32-channel shielded cap while the participants were seated (ANT Neuro, Enschede, Netherlands), as shown in Figure 1. All 32 gel-based sensors were attached to an EEG head eegosports cap, referenced to CPz, and grounded at AFz, as recommended by the manufacturer. The impedances were kept below 10 kΩ.

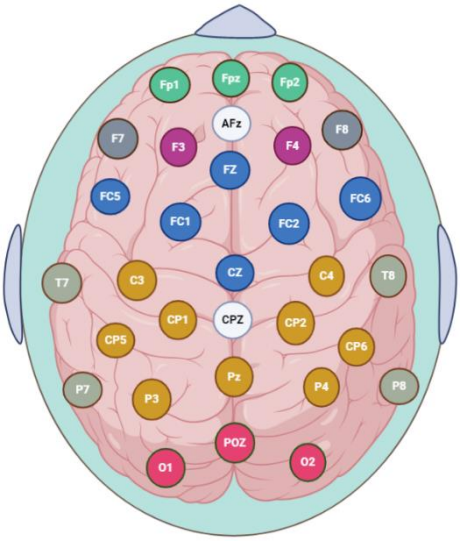

Figure 1. Topographical placement of 31 electrodes using the extended international system 10-20, indicating the distribution of the electrodes on the cortical scalp, categorized as follows: prefrontal (Fp1, Fp2), medial prefrontal (mPFC: Fpz), ventrolateral prefrontal (F7, F8), dorsolateral prefrontal (F3, F4), frontal (FC5, FC1, FC2, FC6), midfrontal (Fz, Cz), temporal (T8, P7, P8), parietal (C3, C4, C3, P8), midparietal (Pz), occipital (O1, O2), and midoccipital (POz).

Preprints (www.preprints.org) | NOT PEER-REVIEWED | Posted: 26 February 2021 doi:10.20944/preprints202102.0610.v1

Recorded electrophysiological data from every channel were digitized at a sampling rate of 2048 Hz and resampled offline to 256 Hz. Raw EEG signals were preprocessed offline to eliminate unnecessary data (noised segments) using BESA Research Toolbox 6.0. To eradicate the high-frequency electrocortical artifacts, signal contamination, and low-frequency deflections, we applied a bandpass filter to obtain the optimal segments between the low and high frequencies (0.4–50 Hz) [35]. Artifacts such as blinking, horizontal and vertical eye motions (HEOG and VEOG, respectively), breathing, power interference, and cardiac movements were visually inspected and automatically discarded using BESA-based artifact-based spatial detection and brain signal topography [36]. The open-source toolboxes also include EEGLAB for the visualization of topographic maps [37]. According to the standardized frequency bands, the data observations and segments were divided into the following ranges: delta (1–3 Hz), theta (4–8 Hz), alpha (8–12 Hz), low beta (13–21 Hz), and high beta (22–30 Hz). To prevent non-stationary confusion, we segmented the data into approximately stationary nonoverlapping short time-series data. The total quantity was 29 epochs (116 s), which was within the domain of a previous resting-state analysis [38], to achieve a balance between the stationarity and the model order fit, as longer time series support more accurate parameter estimation for locally appropriate linear autoregressive models. For our data, we found that shorter segments (1–2 s) negatively affected the model fit for many segments [39]. The EC was calculated based on the localized EEG data (section 2.4) for each segment and then averaged to have one PDC matrix for every subject with (8 (channels) × 8 (channels) × 5 (bands)).

Generally, an MVAR model with a number of cortical DMN regions (*m* electrodes) of EEG signals and order p is defined as follows:

$$\mathrm{X}(t) = \sum_{\mathrm{r}=1}^{\mathrm{p}} A\,(r)\,\mathrm{X}\,(t-r) + \mathrm{E}(t), \tag{1}$$

where

$$\mathrm{Al}=\begin{bmatrix} a_1(l) & \cdots & a_{1n}(l) \\ \vdots & \ldots & \vdots \\ a_n(l) & \ldots & a_{nn}(l) \end{bmatrix}, \tag{2}$$

is the coefficient matrix at the time lag (*l*). X (*t*) represents the weight vector of m electrodes of EEG signals at time t, matrix A (*r*) indicates the rth order AR parameters, and E (*t*) represents the measured error that is believed to be an independent Gaussian process with zero mean.

When the coefficients of the MVAR model are adequately calculated, A (*F*) is determined as follows:

$$\mathrm{A}(F) = \sum_{\mathrm{r}=1}^{\mathrm{p}} \mathrm{A}(r)\mathrm{e}^{-i2\pi fr}, \tag{3}$$

Therefore, the PDC value from channel j to channel i can be expressed as follows:

$$\mathrm{PDC_{ij}}\,(f) = \frac{A_{ij}\,(f)^{-}}{\sqrt{aj^{-H}\,(f)\mathrm{aj}^{-}(f)}}, \tag{4}$$

where, āi (*f*) (*i* = 1, 2, …*M*) represents the ith column of the matrix Ā(f) and PDC*ij* represents the directional influence and intensity of the information flow from channel *j* to channel *i* at a frequency of *f*. The PDC values were computed for each combination and used as an input feature for the classifiers. Features from these frequency bands were chosen to provide optimum accuracy with optimal order at *p* = 5 [40].

2.4. EEG Source Localization-Based effective Connectivity

Preprints (www.preprints.org) | NOT PEER-REVIEWED | Posted: 26 February 2021 doi:10.20944/preprints202102.0610.v1

The acquired EEG signals can be used to perform the inverse problem to define the locations of the predominant sources of the brain activity. To provide more validity to this approach, an additional source localization analysis of all frequency oscillations (0.4–50Hz) in resting state was performed using exact low-resolution brain electromagnetic tomography (eLORETA) in search of the active sources generating the scalp potentials [41]. The eLORETA mechanism is a discrete, three-dimensional distributed, linear, weighted minimum norm inverse solution and has the ability to reconstruct intercortical activity with correct localization from scalp EEG data [42], [43]. Additional merit of eLORETA is that it has no localization bias even in the existence of noise [44]. The exact locations of the EEG signal generators can be restrained to the cortical surface and their orientations of dipole sources restrained to be vertical to the local cortical surface [45]. Generally, the source model of eLORETA estimates the information about the orientation of dipole sources. In this work, we applied a moving window with 1s (time scale) to strengthen the revelations of modulations in different cortical regions, as reported in earlier MEG and EEG works [46], [47]. The time source electrical potentials acquired from the localized EEG signal waveforms were then exported as mean activity in the EC analysis. Through our analysis, it has been found that a set of eight operationally active cortical areas indexed by four distinct: PCC/Precuneus (PZ, P3 and P4), mPFC/vmPFC (FZ, F3, and F4), and LPC (Angular Gyrus and Supramarginal Gyrus (CP5 and CP6)) [48], [49]–[52], is dominant and active in all subjects more than the other cortical areas of the brain. Then, the intercortical surfaces were parcellated into 15000 anatomical vertices on the basis of Montreal Neurological Institute (MNI) templates and Talairach coordinates [35], [53].

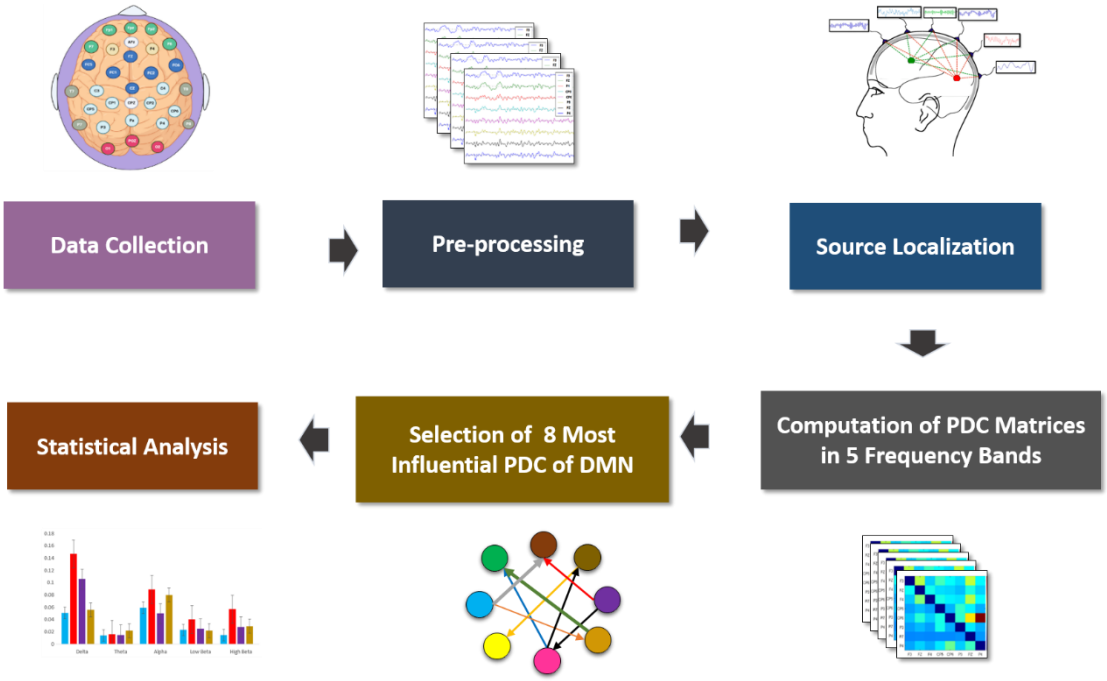

Figure 2. Block diagram for the EEG data analysis module to identify the parameters of the effective connectivity network between DMN regions

We have excluded the non-active cortical areas from any further EC analysis. Table 2 shows the most active EEG regions which could, in large, account for DMN network. EC weights between these active regions were calculated for each artifact-free EEG segment in the mentioned frequency bands. For each subject included in our analysis, we repeated the foregoing procedure to produce the final average PDC for each group from the localized data. Throughout the analysis, the optimum model order for each subject

Preprints (www.preprints.org) | NOT PEER-REVIEWED | Posted: 26 February 2021 doi:10.20944/preprints202102.0610.v1

from Akaike information criterion (AIC) varied from 4 to 10 [54]. The averaged EC (PDC values) for all pairwise electrodes of all the frequency wave connections in the SAD groups exhibited the pairwise relationship between any two electrodes within the network. The entire process is shown in Figure 2.

Table 2. EEG electrodes, default mode network region underneath and MNI coordinates with Brodmann areas and functions.

ROI	MNI coordinates			Anatomical regions	BA	Function
	x	*y*	*z*			
FZ	0.6	40.9	53.9	Central mPFC	8-9-10	Attention [55]
F3	-35.5	40.9	32.1	Left mPFC	8-9-10	Executive control of behavior [56]
F4	40.2	47.6	32.1	Right mPFC	8-9-10	Memory and decision making [57]
PZ	0.2	−62.1	64.5	PCC/ Precuneus	7	Pain perception & goal processing [58]
P3	−39.5	−76.3	47.4	Left LPC	39–40	Theory of mind [59]
P4	38.8	−74.9	49.2	Right LPC	39–40	Recognition and working memory [60]
CP5	−62	−42	32	Left supramarginal cortex	40	Visuospatial processing [61]
CP6	66	−34	40	Right supramarginal cortex	40	Planning and motor imagery [62]

2.5. Clinical Assessment

SIAS reveals and quantifies the approximate fears of more general social interaction and is in accordance with the Social Phobia-Circumscribed DSM-III-R definitions. The SIAS scale has been shown to have high internal consistency levels and reliability for testing-retests. SIAS may distinguish between social phobia, agoraphobia, and simple samples of phobia, as well as between social phobia and common samples [63], [64].

The scale is found to change with medication and stabilize over no-treatment. Furthermore, the SIAS scale tends to be accurate, useful, and valid and easily scored for clinical and research applications, because it exhibits an improvement over existing SAD measures [65]. The SIAS measure is intended to recognize two distinctly different aspects of SAD, including apprehension, escaping daily social interactions, internal fear, and avoidance of performing experiences linked with the perception of sociscrutiny (e.g., dining, consuming food and drinks in public, and writing in the company of others) and more general engagements (e.g., attending or organizing events or making new friends). Indeed, a recent systematic review [66] revealed that the SIAS scale has obtained higher positive scores for the psychometric accuracy than other social evaluation measures. Four subdomains (control, mild, average, and severe) were measured with the 20 questions. The total scores in each subdomain ranged from 1 to 4, with higher scores exhibiting a higher severity of SAD [67].

2.6. Statistical analysis

The distribution of the information flow measurements was assessed with the univariate ANOVA test, and the statistical findings are reported by F values. All the statistical findings were presented as the mean ± standard deviation. The analysis of mean variances in our study included two independent variables (Group: severe, moderate, mild, and control) * (Regions; F3, F4, FZ, CP5, CP6, P3, P4, and PZ)* and one dependent variable (PDC values)); therefore, a one-way Univariate ANOVA and Tukey's HSD post-hoc test for different comparisons ($p < 0.05$) was performed to evaluate the main differences between the causal information flow of frequency EEG data of SAD groups. The relationship

Preprints (www.preprints.org) | NOT PEER-REVIEWED | Posted: 26 February 2021 doi:10.20944/preprints202102.0610.v1

between the SIAS scores and PDC values (PDC values * SIAS scores) in all frequency bands was investigated by Pearson correlation test [68]. The SPSS software (version 25.0.0.0, IBM Corp., Armonk, NY) was used for all the statistical analyses.

3. Results

The experimental findings are presented in the following three subsections: the subjective analytics, the EEG-based EC metrics, and the correlation analysis between the DMN values and SIAS scores.

3.1. Subjective data analysis

Initially, we examined the self-report questionnaire data to determine the group differences between the 4 groups. The total calculated percentages of the SAD groups—control, mild, average, and severe—were 18.38%, 27.09%, 26.12%, and 28.38%, respectively. The participants' responses in the questionnaires were subjected to an analysis of variance (ANOVAs) and the nonparametric test (Mann–Whitney) for parameters that were not normally distributed. However, the analysis did not exhibit any group differences, $F(1, 87) = 2.664$, $p = 054$, $\eta\ 2 = 0.093$. Compared to all groups, severe participants have exhibited significantly higher SAD scores during the experiment: $F(1, 87) = 21.06$, $p = 0.001$, $\eta\ 2 = 0.53$.

3.2. Effective Connectivity in Different Frequency Bands

EC analysis was performed on artifact-free time series with smaller frequency rates to calculate the mean EEG activation in three DMN source-localized brain areas (PCC/Precuneus, LPC, and mPFC/vmPFC). In the first experiment, the EC was calculated over the control, mild, average, and severe SAD groups and averaged within the subjects of each group. Then, the EC values were filtered into the different frequency rhythms (delta, theta, alpha, low beta, and high beta), as shown in Figure 4. The results in Figure 4 indicate the significant difference among the four SAD groups (severe, average, mild, and control); in the delta and alpha bands: $F(3, 252) = 3.937$, $p < 0.009$, $\eta\ 2 = 0.1$ and $F(3, 252) = 3.766$, $p < 0.01$, $\eta\ 2 = 0.1$, respectively. In contrast to the alpha and delta bands, no significant differences were observed in the high beta ($F(3, 252) = 1.571$, $p < 0.196$, $\eta\ 2 = 0.04$) and low beta ($F(3, 252) = 0.410$, $p < 0.746$, $\eta\ 2 = 0.04$) bands. In the delta band, post-hoc testing revealed significant 0.1466, SD = 0.3057) and mild (M = 0.1064, SD = 0.1586), while the control and severe groups exhibited less effective connections of (M = 0.0563, SD = 0.0512) and (M = 0.0514, SD = 0.1052), respectively were observed in the high beta ($F(3, 252) = 1.571$, $p < 0.196$, $\eta 2 = 0.1$) and low beta ($F(3, 252) = 0.410$, $p < 0.746$, $\eta\ 2 = 0.1$) bands. This suggests that there were stronger connections among the DMN regions in the average and mild groups compared with the severe and control groups. Table 3 shows the ANOVA test between the SAD groups and HCs.

Table 3. ANOVA comparisons between PDC values and SAD groups.

Band	Independent variables	F	P value	η 2
Delta	SAD Groups	3.937	0.009	0.1
Theta	SAD Groups	2.389	0.069	0.05
Alpha	SAD Groups	3.766	0.001	0.1
Low beta	SAD Groups	0.410	0.196	0 .04
High beta	SAD Groups	1.571	0.746	0 .04

Moreover, in the alpha band, post-hoc testing revealed significant differences in the EC strengths between the groups; severe (M = 0.0587, SD = 0.0466), average (M = 0.0776, SD = 0.0707), control (M = 0.0797, SD = 0.0641), mild (M = 0.0501, SD = 0.0529). This indicates a stronger alpha connection in severe, average, and control groups more than mild

Preprints (www.preprints.org) | NOT PEER-REVIEWED | Posted: 26 February 2021 doi:10.20944/preprints202102.0610.v1

group. Furthermore, the results indicated significant differences in the theta band between the severe and HC groups for F (3,252) = 2.389, $p < 0.05$, $\eta 2 = 0.1$, (M = 0.0141, SD = 0.0098), (M = 0.0216, SD = 0.0209), respectively. However, the results revealed no significant difference between the rest of the groups, F (3, 252) = 2.389, $p < 0.069$, $\eta 2 = 0.1$, average (M = 0.0163, SD = 0.0024), and mild (M = 0.0147, SD = 0.0024). As mentioned previously, the high beta and low beta did not exhibit any significant differences between any groups ((3, 252) = 1.571, $p < 0.196$, $\eta 2 = 0.1$), F (3, 252) = .410, $p < .746$, $\eta 2 = 0.1$). In the high beta band, the mean EC values were as follows: severe (M = 0.0242, SD = 0.0200), average (M = 0.0371, SD = 0.0515), mild (M = 0.278, SD = 0.034), and differences between the two different groups of average (M = control (M = 0.291, SD = 0.0356). In the low beta band, the mean EC values were as follows: severe (M = 0.23, SD = 0.0172), average (M =0.251, SD = 0.0286), mild (M = 0.254, SD = 0.0244), and control (M = 0.022, SD = 0.0178). Figure 3 presents the distribution of the EC over the DMN regions at the different EEG bands. Clearly, the precuneus region exhibited the strongest EC among the DMN regions.

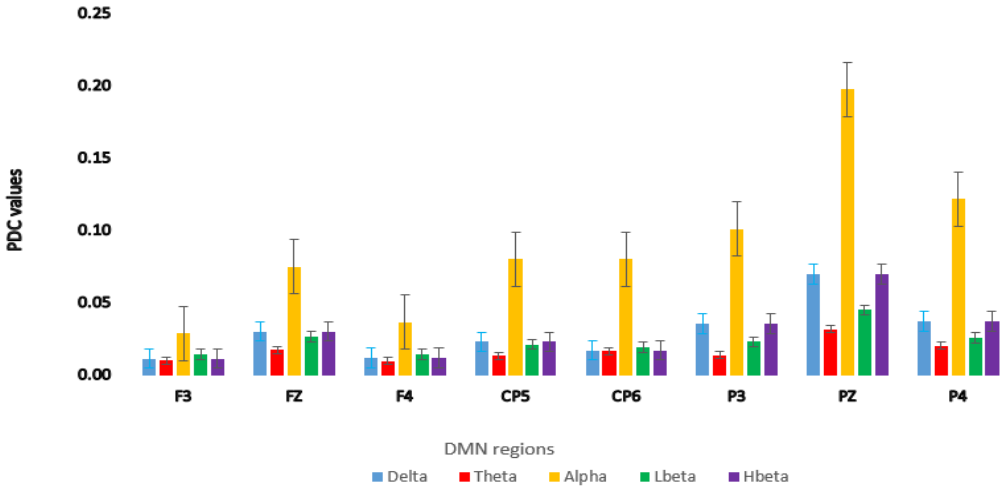

Figure 3. Relationship between the average PDC values and the regional DMN areas.

The topographic mapping of averaged mean EC values at the various DMN regions during the resting-state are shown at different EEG bands in Figure 4. The results indicated greater EC values in the alpha and delta frequency bands in DMN regions compared with the other frequency bands for all four groups. Among the DMN regions, the delta and alpha bands were higher in the LPC and precuneus than in the other DMN regions, in agreement with previous findings [69]. Therefore, the PCC/precuneus is suggested to be a major source hub that contributes to the function and mechanism of cognitive exploration and emotional states of SAD. Apart from that, whole brain connectivity was calculated for more validity, the DMN electrodes were more active than the others in all frequency bands (PDC calculation is attached in supplementary file).

Preprints (www.preprints.org) | NOT PEER-REVIEWED | Posted: 26 February 2021 doi:10.20944/preprints202102.0610.v1

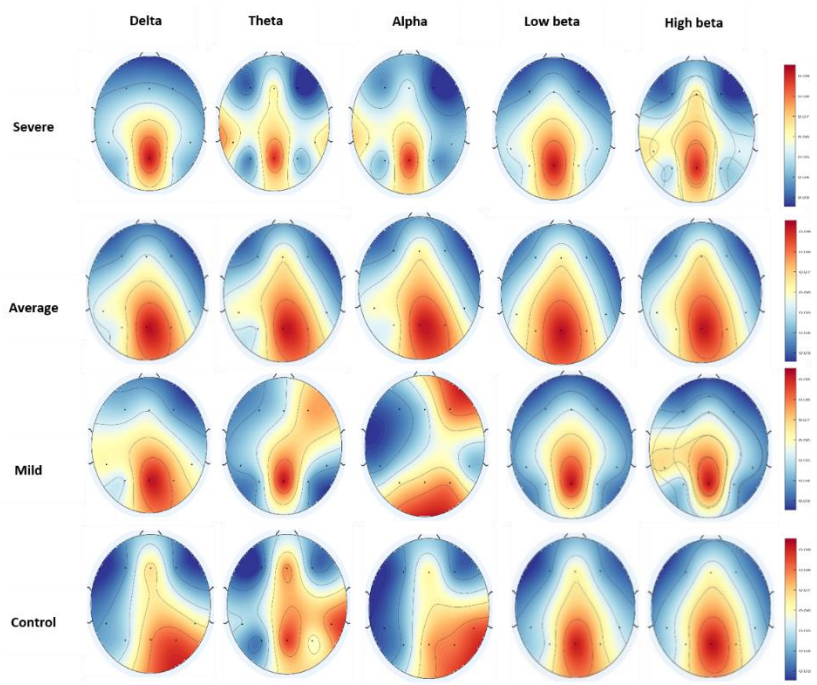

Figure 4. Topological maps of the mean total information flow for all four SAD groups in the frequency bands. Red indicates greater PDC values; blue indicates a smaller PDC.

3.3. Pairwise EC of DMN components in SAD

In this section, the heat-map of the average EC over each group is constructed. This map is represented in matrix form, where the entry (i, j) indicates the causal influence of the j-region on i-region at a certain band. The values of the heat map are displayed in a color scale, where the blue represents the minimum range of the EC values, and the red represents the maximum range. In the delta band, the severe group exhibited more information flows in the right hemisphere (LH) than in the left hemisphere (RH) between the precuneus sides and mPFC; the LPC and mPFC (PZ→F4); (CP5→ F4), from precuneus where the mPFC only receives the information as shown in Figure 7. Greater information flows in the RH compared with the LH were detected in the LPC and right mPFC regions (P4→F4 and PZ→F4), right LPC (P4→CP6), and mPFC (FZ→F4). In the case of the mild group, the enhanced information flow in RH was higher than that in LH between the precuneus sides (F3, PZ and P4), and (PZ→F3 and P3→F3); (F4→F3 and (P4→F4). The HC has exhibited greater information flow from RH to LH (P4→CP5). Additionally, in the alpha, there were more significant differences in EC in the RH than in the LH with long-domain correlation in the precuneus and right LPC regions for the average and mild groups (PZ→F4, FZ→F4 and P3→CP6): (PZ→F3, PZ→F4 and PZ→CP6), whereas the HC group exhibited a larger quantity of causal information flow in the LH than in the RH in the left LPC and mPFC sites (CP5→P3, FZ→F3 and P3→CP5).

In comparison, smaller amounts of information flow within the left LPC region (CP5→P3 and P4→CP6) were observed for the severe group. However, the theta band exhibited a smaller flow of information between the precuneus and the mPFC (PZ→F4) and LPC (CP6→P3) for the HC group than for the severe group. Compared with the average group, mild participants exhibited a greater flow of information between the precuneus, LPC, and mPFC (P→ F4, PZ→F3, and PZ→CP5). Within the high beta band, the HC group exhibited greater information transmission between the LPC and the precuneus regions (PZ→CP5) in the LH. Thus, the HC subjects experienced more robust EC than the severe group. In addition, for the average group, there was enhanced information flow in the RH relative to the LH at the precuneus and rLPC (PZ→CP6, P4→CP6). Similarly, for the mild

Preprints (www.preprints.org) | NOT PEER-REVIEWED | Posted: 26 February 2021 doi:10.20944/preprints202102.0610.v1

class, there was a significant amount of information flow in the RH (PZ→F4). Lastly, the high beta band exhibited greater information flow than the low beta band. Firmly, the changes in EC between the DMN regions in the SAD patients suggested enhanced regulation by the neural system of the SAD, compared with the findings for the HC group. These results indicate that the abnormal EC between the DMN regions was related to a brain-function change in SAD. Figure 5 illustrates the significant differences in the average absolute EC in both brain hemispheres for electrode paired connections. Figure 6 has proven that precuneus is the pivotal hub of the DMN in severe and moderate SAD groups compared to HC and mild groups. HC individuals have shown higher EC in the mPFC region compared to the other groups, which indicates higher cognitive functions. Mild and moderate groups have shown greater information flow in the left mPFC than the other groups. The data shown in Figure 6 is obtained from the alpha band due to its ability to explore mental illness and emotional states.

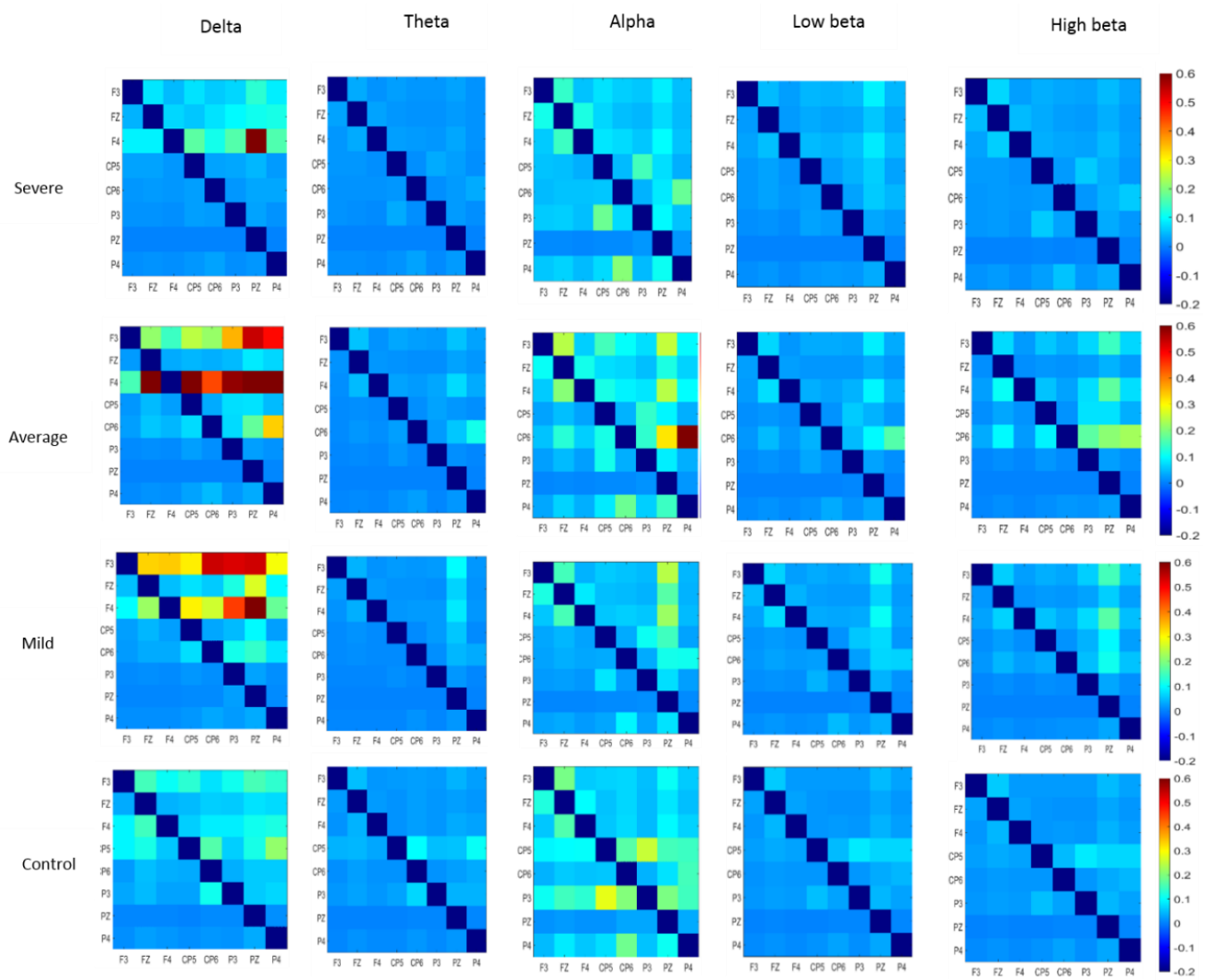

Figure 5. Mean EC intensity matrices of eight DMN neuronal clusters in the resting state. Every component in the matrix represents the mean EC magnitudes for all participants. The information flow can be represented by the flow from the lower rows to the left columns. The red color of the components reflects the greater EC significance of the connectivity. Diagonal values are set as zero.

Preprints (www.preprints.org) | NOT PEER-REVIEWED | Posted: 26 February 2021 doi:10.20944/preprints202102.0610.v1

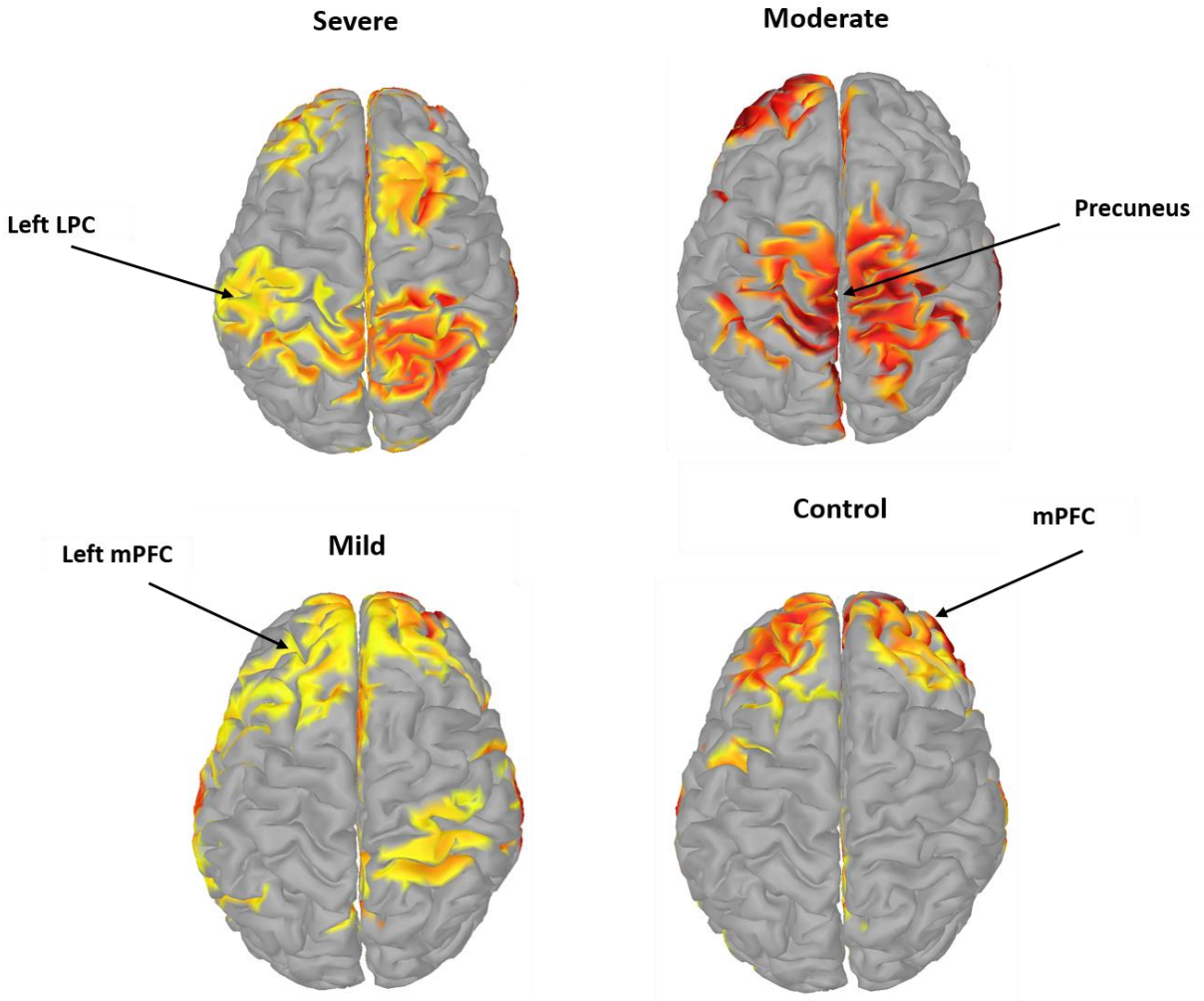

Figure 6: A 3D visualization of the computed EC source from EEG activity at the alpha band. It represents the highest 20% values at a threshold of significant level $p < 0.05$.

3.4 Correlation analysis between EC values and self-report measures

The Pearson correlation coefficient was used to evaluate the linear correlation between the total averaged EC connectivity values (PDC values) in the DMN and the self-report questionnaire SIAS. Behaviorally, the severe group exhibited a positive significance correlation between the DMN and SIAS scores, i.e., $r(22) = 0.576$, $p = 0.006$, as shown in Figure 6. The correlation between the DMN and SIAS scores was negative for the control group, i.e., $r(22) = -0.689$, $p = 0.001$. The mild and average groups did not exhibit any significance in the correlation, $r(22) = 0.168$, $p = 0.491$, $r(22) = -0.326$, $p = 0.149$, respectively. Figure 9 show all the correlations between the SAD groups in alpha band, due ti its influence in brain disorders [70].

Preprints (www.preprints.org) | NOT PEER-REVIEWED | Posted: 26 February 2021 doi:10.20944/preprints202102.0610.v1

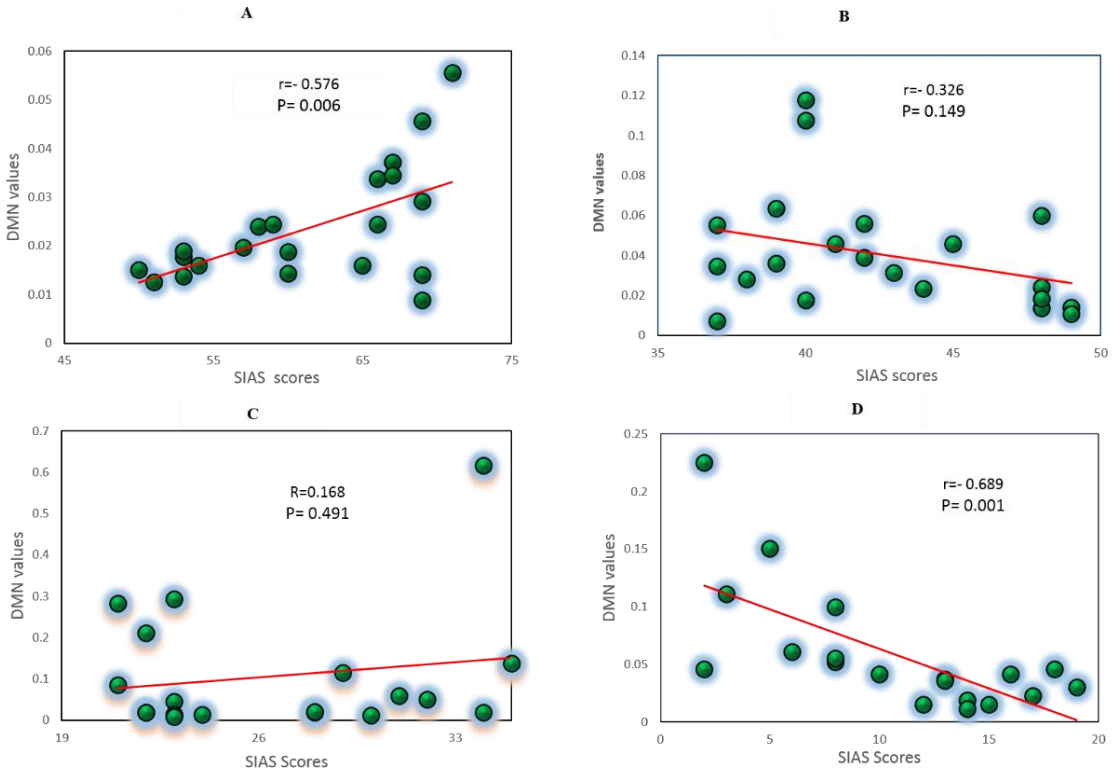

Figure 6. Correlation between the DMN EC and SIAS scores for the SAD groups, severe (A), moderate (B), mild (C), and control (D).

4. Discussion

To the best of our knowledge, this was the first study in which the EEG-based EC was used to segregate the severity of SAD by categorizing its grading (control mild, average, and severe) and investigate the neurocorrelates characteristics of the DMN resting state and the topological organization of the effective brain connectivity network in SAD. The results in Section 3 indicate significant values for the EC among all the SAD groups in the dominant frequencies at rest, i.e., the delta and alpha bands. This finding agrees with previous studies on the DMN [71]. In the theta band, the results exhibited enhanced frontal midline interconnectivity and greater causal effects for the control group than for the severe group at the precuneus and LPC. However, in the theta band, we observed a tendency of enhanced frontal midline neuroconnectivity and greater causal connections in severe SAD and HC relative to the average and mild groups. Additionally, the DMN connectivity amplitudes were negatively correlated to the SIAS state anxiety within the control group. The SIAS scores of the individuals with SAD exhibited a positive significant correlation with the mean DMN values. We observed a significant difference in the effective connectivity intensities for all the SAD categories at the low frequency band (delta).

The ANOVA test in the ROI analysis revealed significantly greater EC values in the precuneus than in all other ROIs [72]. Moreover, the findings reveal that the precuneus is more active when individuals with SAD are in the resting-state (absent of any external stimulus), and it is implicated in a neural network of self-awareness, autobiographical tasks [73] , cognitive interpretation, and future planning [74]. Thus, our study provided empirical evidence that the precuneus dysfunction in the SAD yields an imprecise interpretation of the inner-emotional status as well as deficient processing of inner self-repre-

 doi:10.20944/preprints202102.0610.v1

sentation [75]. We believe that the dysfunction of the precuneus in the DMN of SAD individuals may be related to the development of SAD symptoms as well as to the high-level maintenance of self-focused attention [25]. The precuneus activity is enhanced during self-processing and perception (resting state) and reduced during goal-directed, non-self-referential tasks (performing task) [76]. Reduced activity in DMN brain areas (which was observed more frequently in our SAD subjects compared with HC individuals) may indicate a continued need to maintain self-focused awareness during a resting-state, presumably owing to the utilization of higher motivational pertinence to the anticipation of the next tasks in our experiment.

Interestingly, statistical findings revealed that relative to the HC group, the SAD patients exhibited differences in EC neurocorrelates in the mPFC. The right mPFC activation was higher for the severe group. In comparison to severe group, the HC group exhibited a stronger correlation between the precuneus and the mPFC. This suggests that the changes in EC between the precuneus and the mPFC may have had a structural basis. Additionally, the severe group exhibited stronger causal activation in the mPFC and greater inhibition in the LPC in the DMN compared with the HC group. Previously, SAD patients exhibited increased activity within the left mPFC when performing a mental arithmetic task [77]. Our findings provide evidence of mPFC dysfunction in SAD patients and suggest that mPFC dysfunction may contribute to disparities within SAD categories. Neuroscientists believe that the increased inhibition of mPFC may reflect aberrant regulation of the neural mechanism in patients with SAD [78]. In the antecedent studies, the activity in the mPFC of SAD subjects had inconsistent findings about the neural activation (increased or decreased) in the resting-state but exhibited a significant difference in the performance of the cognitive tasks in the DMN areas [18], [75]. The activity of the mPFC possibly reflects the neurocorrelates between cognitive behavioral processing and emotional states in positron-emission tomography [79], [17]. Our results, together with the hypotheses on mPFC, indicate that mPFC plays a significant role in the influential psychopathology mechanism of SAD. Therefore, the mPFC may be engaged in the internal reflection of the social world [80] and plays a major role in the capacity to interpret certain mental states (e.g., cognitive function) [81]. The mPFC-precuneus dysfunction in this finding may represent the dysfunction of cortical regions that directly contribute to the pathophysiology of SAD. Our findings on the mPFC have not been reported previously.

While many studies have revealed an aberrant resting state EC in different distant brain networks in SAD, to the best of our knowledge, no resting-state EEG study has been performed on the severity of SAD in DMN using EC. Our results also indicated that the EC of the mPFC regions in the DMN involved in self-referential and emotional processes exhibited stronger connectivity in the severe group, whereas the LPC sites of the DMN which were implicated in episodic memory and visual processing exhibited stronger connectivity in the HC group compared with the severe group. These findings are consistent with previously reported results of LPC and DMN research [82]. Dissociation between the mPFC and cortical midline LPC regions leads to the possibility of a behavioral differentiation within the DMN in terms of self-referential functions and contributes to the comprehension of perceptual and affective changes in SAD. The LPC exhibited a reduced and anomalous interaction in the SAD patients compared with the HC group, suggesting greater behavioral avoidance for the SAD participants as reported in [82]. These behaviors have been proven to intermediate introspection and reflection upon one's own mental state in HC [83]. Thus, we consider that the increased inhibition of the precuneus-mPFC for the severe group can be linked to the deviant regulation of fear, whereas the reduced inhibition of the precuneus-LPC for the HC is linked to the impairment of autobiographical memory, as reported in a previous work [78]. Table 4 is presenting the most relevant literature to our study. Compared to the exist literature about DMN activities in SAD individuals, our study is the first to investigate the severity of SAD (severe, moderate, mild, and HC) with sufficient dataset (88 subjects) and exact localization of EEG sources. Our findings are in line with many fMRI studies that showed aberrant connectivity between DMN regions in resting-state.

Preprints (www.preprints.org) | NOT PEER-REVIEWED | Posted: 26 February 2021 doi:10.20944/preprints202102.0610.v1

Table 4. A comparison between the current study and relevant studies in literature.

Ref	Method	Network	No. subjects	Main findings
[21]	fMRI	DMN	84	Increased DMN activity in PCC and LPC.
[23]	fMRI	Salience network & DMN	12	DMN connectivity was not different between groups.
[26]	fMRI	DMN	8	SAD showed higher activation in the precuneus than HCs.
[84]	fMRI	DMN	40	The FC in the right precuneus had decreased in SAD patients as compared to HC.
[85]	EEG	DMN	47	SAD individuals showed a decrease of FC between mPFC and PCC.
This study	EEG	DMN	88	Enhanced EC between the DMN regions in SAD patients compared to HCs in resting-state.

This study had limitations. First, the SAD participants were adults, and the comorbidity of other possible psychiatric disorders was not identified. The existence of comorbidities may have affected the findings, which requires further investigation. Second, the findings are focused on the SAD population and should not be extended to other psychological disorders or internalization issues. Third, it has also been reported that the EC [86] cannot capture inhibitory connections with the same accuracy as excitatory connection and was not accurate for discriminating between mono-and poly-synaptic interconnections; thus, the findings reported herein may be validated with other connectivity algorithms. Forth, we only concentrated on EEG signals in DMN areas; future EC research should focus on different brain modalities and regions, such as the fMRI subcortical regions. Finally, our research was a cross-sectional analysis; thus, only the resting state was investigated. Further studies would benefit from a retrospective approach.

5. Conclusions

This study was the first investigation of the DMN EC network for SAD in different frequency bands. The use of directed EC estimates was suggested, and networks were identified via PDC analysis to evaluate the effect of SAD in DMN brain areas. Therefore, our findings indicated that individuals with SAD not only had abnormal alteration processing of certain socially anxious triggers but also exhibited stronger disturbance emotion processing in the basic nervous system pathway. The results reported herein are useful for the development of cognitive therapy models and the treatment of SAD. We reported a discriminatory deterioration or abnormality in the neural activity of the precuneus, mPFC, and LPC in severe SAD patients. It is believed that these regions with abnormal activations are biomarkers of SAD, representing the rudimentary pathophysiology and deficiency in the SAD groups. Overall, the subjective and electrophysiological findings indicate that EEG observations of the effects of SAD on emotional and cognitive processes in the DMN can serve as early biomarkers for SAD diagnosis and treatment.

Acknowledgment

This research was supported by the Ministry of Education, Malaysia under the Higher Institute Centre of Excellence (HiCOE) scheme awarded to the Centre for Intelligent Signal and Imaging Research (CISIR), Universiti Teknologi PETRONAS

References

[1] C. A. Brook and L. A. Schmidt, "Social anxiety disorder: A review of environmental risk factors," *Neuropsychiatric Disease and Treatment*, vol. 4, no. 1 A. Dove Press, pp. 123–143, 2008.

[2] K. Golombek, L. Lidle, B. Tuschen-Caffier, J. Schmitz, and V. Vierrath, "The role of emotion regulation in socially anxious children and adolescents: a systematic review," *European Child and Adolescent Psychiatry*. Dr. Dietrich Steinkopff Verlag GmbH and Co. KG, pp. 1–23, 14-Jun-2019.

[3] S. G. Hofmann, "Cognitive factors that maintain social anxiety disorder: A comprehensive model and its treatment implications," *Cogn. Behav. Ther.*, vol. 36, no. 4, pp. 193–209, 2007.

[4] M. Modini and M. J. Abbott, "A comprehensive review of the cognitive determinants of anxiety and rumination in social anxiety disorder," *Behav. Chang.*, vol. 33, no. 3, pp. 150–171, Sep. 2016.

[5] A. B. Brühl, A. Delsignore, K. Komossa, and S. Weidt, "Neuroimaging in social anxiety disorder-A meta-analytic review resulting in a new neurofunctional model," *Neuroscience and Biobehavioral Reviews*, vol. 47. Elsevier Ltd, pp. 260–280, 01-Nov-2014.

[6] A. Al-Ezzi, N. K. Selman, I. Faye, and E. Gunaseli, "Electrocortical brain oscillations and social anxiety disorder: a pilot study of frontal alpha asymmetry and delta-beta correlation," *J. Phys. Conf. Ser.*, vol. 1529, p. 052037, May 2020.

[7] Y. Chen *et al.*, "Abnormal dynamic functional connectivity density in patients with generalized anxiety disorder," *J. Affect. Disord.*, vol. 261, pp. 49–57, Jan. 2020.

[8] J. Ding *et al.*, "Disrupted functional connectivity in social anxiety disorder: A resting-state fMRI study," *Magn. Reson. Imaging*, vol. 29, no. 5, pp. 701–711, Jun. 2011.

[9] K. Golombek, L. Lidle, B. Tuschen-Caffier, J. Schmitz, and V. Vierrath, "The role of emotion regulation in socially anxious children and adolescents: a systematic review," *European Child and Adolescent Psychiatry*. Dr. Dietrich Steinkopff Verlag GmbH and Co. KG, 14-Jun-2019.

[10] R. Sladky *et al.*, "Disrupted effective connectivity between the amygdala and orbitofrontal cortex in social anxiety disorder during emotion discrimination revealed by dynamic causal modeling for fMRI," *Cereb. Cortex*, vol. 25, no. 4, pp. 895–903, 2013.

[11] J. Manning *et al.*, "Altered resting-state functional connectivity of the frontal-striatal reward system in social anxiety disorder," *PLoS One*, vol. 10, no. 4, Apr. 2015.

[12] F. Liu *et al.*, "Disrupted cortical hubs in functional brain networks in social anxiety disorder," *Clin. Neurophysiol.*, vol. 126, no. 9, pp. 1711–1716, Sep. 2015.

[13] E. Kuru *et al.*, "Cognitive distortions in patients with social anxiety disorder: Comparison of a clinical group and healthy controls," *Eur. J. Psychiatry*, vol. 32, no. 2, pp. 97–104, Apr. 2018.

[14] H. Crawford *et al.*, "A Behavioural Assessment of Social Anxiety and Social Motivation in Fragile X, Cornelia de Lange and Rubinstein-Taybi Syndromes," *J. Autism Dev. Disord.*, vol. 50, no. 1, pp. 127–144, Jan. 2020.

[15] A. Al-Ezzi, N. Kamel, I. Faye, and E. Gunaseli, "Review of EEG, ERP, and Brain Connectivity Estimators as Predictive Biomarkers of Social Anxiety Disorder," *Frontiers in Psychology*, vol. 11. Frontiers Media S.A., 19-May-2020.

[16] C. Qiu *et al.*, "Regional homogeneity changes in social anxiety disorder: A resting-state fMRI study," *Psychiatry Res. - Neuroimaging*, vol. 194, no. 1, pp. 47–53, Oct. 2011.

[17] R. L. Buckner, J. R. Andrews-Hanna, and D. L. Schacter, "The brain's default network: Anatomy, function, and relevance to disease," *Annals of the New York Academy of Sciences*, vol. 1124. Ann N Y Acad Sci, pp. 1–38, Mar-2008.

[18] X. H. Zhao *et al.*, "Altered default mode network activity in patient with anxiety disorders: An fMRI study," *Eur. J. Radiol.*, vol. 63, no. 3, pp. 373–378, Sep. 2007.

[19] Y. Tao *et al.*, "The Structural Connectivity Pattern of the Default Mode Network and Its Association with Memory and Anxiety," *Front. Neuroanat.*, vol. 9, no. November, pp. 1–10, Nov. 2015.

[20] S. A. Anteraper, C. Triantafyllou, A. T. Sawyer, S. G. Hofmann, J. D. Gabrieli, and S. Whitfield-Gabrieli, "Hyper-connectivity of subcortical resting-state networks in social anxiety disorder," *Brain Connect.*, vol. 4, no. 2, pp. 81–90, Mar. 2014.

[21] E. L. Maresh, J. P. Allen, and J. A. Coan, "Increased default mode network activity in socially anxious individuals during reward processing," *Biol. Mood Anxiety Disord.*, vol. 4, no. 1, p. 7, Dec. 2014.

[22] A. B. Brühl, M. Rufer, A. Delsignore, T. Kaffenberger, L. Jäncke, and U. Herwig, "Neural correlates of altered general emotion processing in social anxiety disorder," *Brain Res.*, vol. 1378, pp. 72–83, Mar. 2011.

[23] J. N. Pannekoek *et al.*, "Resting-state functional connectivity abnormalities in limbic and salience networks in social anxiety disorder without comorbidity," *Eur. Neuropsychopharmacol.*, vol. 23, no. 3, pp. 186–195, Mar. 2013.

[24] J. M. Warwick, P. Carey, G. P. Jordaan, P. Dupont, and D. J. Stein, "Resting brain perfusion in social anxiety disorder: A voxel-wise whole brain comparison with healthy control subjects," *Prog. Neuro-Psychopharmacology Biol. Psychiatry*, vol. 32, no. 5, pp. 1251–1256, Jul. 2008.

[25] A. E. Cavanna and M. R. Trimble, "The precuneus: a review of its functional anatomy and behavioural correlates," *Brain*, vol. 129, pp. 564–583, 2006.

[26] C. Gentili *et al.*, "Beyond amygdala: Default Mode Network activity differs between patients with Social Phobia and healthy controls," *Brain Res. Bull.*, vol. 79, no. 6, pp. 409–413, Aug. 2009.

[27] A. Seth, "Causal connectivity of evolved neural networks during behavior," *Netw. Comput. Neural Syst.*, vol. 16, no. 1, pp. 35–54, Mar. 2005.

[28] L. A. Baccalá and K. Sameshima, "Partial directed coherence: A new concept in neural structure determination," *Biol. Cybern.*, vol. 84, no. 6, pp. 463–474, 2001.

[29] M. Kaminski and K. J. Blinowska, "Directed Transfer Function is not influenced by volume conduction-inexpedient pre-processing should be avoided," *Frontiers in Computational Neuroscience*, vol. 8, no. JUN. Frontiers Research Foundation, 10-Jun-2014.

[30] K. J. Blinowska, "Review of the methods of determination of directed connectivity from multichannel data," *Medical and Biological Engineering and Computing*, vol. 49, no. 5. Springer, pp. 521–529, May-2011.

[31] B. J. Ries, D. W. McNeil, M. L. Boone, C. L. Turk, L. E. Carter, and R. G. Heimberg, "Assessment of contemporary social phobia verbal report instruments," *Behav. Res. Ther.*, vol. 36, no. 10, pp. 983–994, Oct. 1998.

[32] F. Faul, E. Erdfelder, A. G. Lang, and A. Buchner, "G*Power 3: A flexible statistical power analysis program for the social, behavioral, and biomedical sciences," in *Behavior Research Methods*, 2007, vol. 39, no. 2, pp. 175–191.

[33] A. P. Association and others, "Diagnostic and statistical manual of mental disorders," *BMC Med*, vol. 17, pp. 133–137, 2013.

[34] JAVA, "Declaration of Helsinki World Medical Association Declaration of Helsinki," *Bull. world Heal. Organ.*, vol. 79, no. 4, pp. 373–374, 2013.

[35] F. Vecchio *et al.*, "Cortical connectivity in fronto-temporal focal epilepsy from EEG analysis: A study via graph theory," *Clin. Neurophysiol.*, vol. 126, no. 6, pp. 1108–1116, Jun. 2015.

[36] P. Sheela and S. D. Puthankattil, "A hybrid method for artifact removal of visual evoked eeg," *J. Neurosci. Methods*, vol. 336, p. 108638, Apr. 2020.

[37] A. Delorme and S. Makeig, "EEGLAB: an open sorce toolbox for analysis of single-trail EEG dynamics including independent component anlaysis," *J. Neurosci. Methods*, vol. 134, pp. 9–21, 2004.

[38] M. Yu *et al.*, "Different functional connectivity and network topology in behavioral variant of frontotemporal dementia and Alzheimer's disease: An EEG study," *Neurobiol. Aging*, vol. 42, pp. 150–162, Jun. 2016.

[39] S. Konda, D. Advisor, and W. A. Woyczynski, "FITTING MODELS OF NONSTATIONARY TIME SERIES: AN APPLICATION TO EEG DATA," 2006.

[40] F. Vaz, P. G. de Oliveira, and J. C. Principe, "A study on the best order for autoregressive EEG modelling," *Int. J. Biomed. Comput.*, vol. 20, no. 1–2, pp. 41–50, Jan. 1987.

[41] R. D. Pascual-Marqui *et al.*, "Assessing interactions in the brain with exact low-resolution electromagnetic tomography," *Philos. Trans. R. Soc. A Math. Phys. Eng. Sci.*, vol. 369, no. 1952, pp. 3768–3784, Oct. 2011.

[42] R. Grech *et al.*, "Review on solving the inverse problem in EEG source analysis," *Journal of NeuroEngineering and Rehabilitation*, vol. 5, no. 1. BioMed Central, p. 25, 07-Nov-2008.

[43] A. Lopez Rincon and S. Shimoda, "The inverse problem in electroencephalography using the bidomain model of electrical activity," *J. Neurosci. Methods*, vol. 274, pp. 94–105, Dec. 2016.

[44] R. D. Pascual-Marqui, "Discrete, 3D distributed linear imaging methods of electric neuronal activity. Part 1: exact, zero error localization," 1985.

[45] A. M. Dale and M. I. Sereno, "Improved localization of cortical activity by combining EEG and MEG with MRI cortical surface reconstruction: A linear approach," *J. Cogn. Neurosci.*, vol. 5, no. 2, pp. 162–176, 1993.

[46] Q. Liu, S. Farahibozorg, C. Porcaro, N. Wenderoth, and D. Mantini, "Detecting large-scale networks in the human brain using high-density electroencephalography," *Hum. Brain Mapp.*, vol. 38, no. 9, pp. 4631–4643, Sep. 2017.

[47] F. De Pasquale *et al.*, "Temporal dynamics of spontaneous MEG activity in brain networks," *Proc. Natl. Acad. Sci. U. S. A.*, vol. 107, no. 13, pp. 6040–6045, Mar. 2010.

[48] H. Koshino, T. Minamoto, K. Yaoi, M. Osaka, and N. Osaka, "Coactivation of the default mode network regions and working memory network regions during task preparation," *Sci. Rep.*, vol. 4, Aug. 2014.

[49] P. Fransson, "Spontaneous low-frequency BOLD signal fluctuations: An fMRI investigation of the resting-state default mode of brain function hypothesis," *Hum. Brain Mapp.*, vol. 26, no. 1, pp. 15–29, Sep. 2005.

[50] M. E. Raichle, A. M. MacLeod, A. Z. Snyder, W. J. Powers, D. A. Gusnard, and G. L. Shulman, "A default mode of brain function," *Proc. Natl. Acad. Sci. U. S. A.*, vol. 98, no. 2, pp. 676–682, Jan. 2001.

[51] M. D. Greicius, G. Srivastava, A. L. Reiss, and V. Menon, "Default-mode network activity distinguishes Alzheimer's disease from healthy aging: Evidence from functional MRI," *Proc. Natl. Acad. Sci. U. S. A.*, vol. 101, no. 13, pp. 4637–4642, Mar. 2004.

[52] D. KHAN, N. Kamel, M. Muzaimi, and T. Hill, "Effective Connectivity for Default Mode Network Analysis of Alcoholism," *Brain Connect.*, Aug. 2020.

[53] J. Mazziotta *et al.*, "A probabilistic atlas and reference system for the human brain: International Consortium for Brain Mapping (ICBM)," *Philosophical Transactions of the Royal Society B: Biological Sciences*, vol. 356, no. 1412. Royal Society, pp. 1293–1322, 29-Aug-2001.

[54] P. A. Valdes-Sosa, A. Roebroeck, J. Daunizeau, and K. Friston, "Effective connectivity: influence, causality and biophysical modeling," *Neuroimage*, vol. 58, no. 2, pp. 339–361, 2011.

[55] D. R. Addis, A. R. McIntosh, M. Moscovitch, A. P. Crawley, and M. P. McAndrews, "Characterizing spatial and temporal features of autobiographical memory retrieval networks: A partial least squares approach," *Neuroimage*, vol. 23, no. 4, pp. 1460–1471, 2004.

[56] K. M. Knutson *et al.*, "Areas of brain damage underlying increased reports of behavioral disinhibition," *J. Neuropsychiatry Clin. Neurosci.*, vol. 27, no. 3, pp. 193–198, Aug. 2015.

[57] D. R. Euston, A. J. Gruber, and B. L. McNaughton, "The Role of Medial Prefrontal Cortex in Memory and Decision Making," *Neuron*, vol. 76, no. 6. Neuron, pp. 1057–1070, 20-Dec-2012.

[58] A. E. Cavanna and M. R. Trimble, "The precuneus: a review of its functional anatomy and behavioural correlates," *Brain*, vol. 129, no. 3, pp. 564–583, Mar. 2006.

[59] Y. Wu *et al.*, "The Neuroanatomical Basis for Posterior Superior Parietal Lobule Control Lateralization of Visuospatial Attention," *Front. Neuroanat.*, vol. 10, no. MAR, p. 32, Mar. 2016.

[60] A. Cañas, M. Juncadella, R. Lau, A. Gabarrós, and M. Hernández, "Working memory deficits after lesions involving the supplementary motor area," *Front. Psychol.*, vol. 9, no. MAY, May 2018.

[61] A. Seydell-Greenwald, K. Ferrara, C. E. Chambers, E. L. Newport, and B. Landau, "Bilateral parietal activations for complex

visual-spatial functions: Evidence from a visual-spatial construction task," *Neuropsychologia*, vol. 106, pp. 194–206, Nov. 2017.

[62] P. Mathew, P. P. Batchala, and T. J. Eluvathingal Muttikkal, "Supplementary Motor Area Stroke Mimicking Functional Disorder," *Stroke*, vol. 49, no. 2, pp. e28–e30, Feb. 2018.

[63] R. G. Heimberg, G. P. Mueller, C. S. Holt, D. A. Hope, and M. R. Liebowitz, "Assessment of anxiety in social interaction and being observed by others: The social interaction anxiety scale and the Social Phobia Scale," *Behav. Ther.*, vol. 23, no. 1, pp. 53–73, Dec. 1992.

[64] Q. J. J. Wong, B. Gregory, and L. F. McLellan, "A Review of Scales to Measure Social Anxiety Disorder in Clinical and Epidemiological Studies," *Current Psychiatry Reports*, vol. 18, no. 4. Current Medicine Group LLC 1, pp. 1–15, 01-Apr-2016.

[65] R. P. Mattick and J. C. Clarke, "Development and validation of measures of social phobia scrutiny fear and social interaction anxiety," *Behav. Res. Ther.*, vol. 36, no. 4, pp. 455–470, Apr. 1998.

[66] N. Wong, D. E. Sarver, and D. C. Beidel, "Quality of life impairments among adults with social phobia: The impact of subtype," *J. Anxiety Disord.*, vol. 26, no. 1, pp. 50–57, Jan. 2012.

[67] M. Modini, M. J. Abbott, and C. Hunt, "A Systematic Review of the Psychometric Properties of Trait Social Anxiety Self-Report Measures," *Journal of Psychopathology and Behavioral Assessment*, vol. 37, no. 4. Springer New York LLC, pp. 645–662, 01-Dec-2015.

[68] P. Schober, C. Boer, and L. A. Schwarte, "Correlation Coefficients," *Anesth. Analg.*, vol. 126, no. 5, pp. 1763–1768, May 2018.

[69] G. G. Knyazev, A. N. Savostyanov, and E. A. Levin, "Alpha oscillations as a correlate of trait anxiety," *Int. J. Psychophysiol.*, vol. 53, no. 2, pp. 147–160, 2004.

[70] J. J. Foxe and A. C. Snyder, "The role of alpha-band brain oscillations as a sensory suppression mechanism during selective attention," *Front. Psychol.*, vol. 2, no. JUL, p. 154, Jul. 2011.

[71] G. G. Knyazev, A. N. Savostyanov, and E. A. Levin, "Alpha oscillations as a correlate of trait anxiety," *Int. J. Psychophysiol.*, vol. 53, no. 2, pp. 147–160, Jul. 2004.

[72] D. M. Amodio and C. D. Frith, "Meeting of minds: The medial frontal cortex and social cognition," *Nature Reviews Neuroscience*, vol. 7, no. 4. Nat Rev Neurosci, pp. 268–277, 16-Mar-2006.

[73] R. N. Spreng, "The Fallacy of a 'Task-Negative' Network," *Front. Psychol.*, vol. 3, no. MAY, p. 145, May 2012.

[74] G. Northoff, A. Heinzel, M. de Greck, F. Bermpohl, H. Dobrowolny, and J. Panksepp, "Self-referential processing in our brain-A meta-analysis of imaging studies on the self," *Neuroimage*, vol. 31, no. 1, pp. 440–457, May 2006.

[75] C. Qiu *et al.*, "Analysis of altered baseline brain activity in drug-naive adult patients with social anxiety disorder using resting-state functional MRI," *Psychiatry Investig.*, vol. 12, no. 3, pp. 372–380, Jul. 2015.

[76] J. F. Coutinho, S. V. Fernandesl, J. M. Soares, L. Maia, Ó. F. Gonçalves, and A. Sampaio, "Default mode network dissociation in depressive and anxiety states," *Brain Imaging Behav.*, vol. 10, no. 1, pp. 147–157, Mar. 2016.

[77] C. D. Kilts *et al.*, "The neural correlates of social anxiety disorder and response to pharmacotherapy," *Neuropsychopharmacology*, vol. 31, no. 10, pp. 2243–2253, Oct. 2006.

[78] F. Chen *et al.*, "Increased Inhibition of the Amygdala by the mPFC may Reflect a Resilience Factor in Post-traumatic Stress Disorder: A Resting-State fMRI Granger Causality Analysis," *Front. Psychiatry*, vol. 9, p. 516, Oct. 2018.

[79] J. R. Simpson, A. Z. Snyder, D. A. Gusnard, and M. E. Raichle, "Emotion-induced changes in human medial prefrontal cortex: I. During cognitive task performance," *Proc. Natl. Acad. Sci. U. S. A.*, vol. 98, no. 2, pp. 683–687, Jan. 2001.

[80] R. Adolphs, "Cognitive neuroscience: Cognitive neuroscience of human social behaviour," *Nat. Rev. Neurosci.*, vol. 4, no. 3, pp. 165–178, 2003.

[81] L. C. Bowman, D. Dodell-Feder, R. Saxe, and M. A. Sabbagh, "Continuity in the neural system supporting children's theory of mind development: Longitudinal links between task-independent EEG and task-dependent fMRI," *Dev. Cogn. Neurosci.*, vol. 40, p. 100705, Dec. 2019.

[82] Y. I. Sheline *et al.*, "The default mode network and self-referential processes in depression," *Proc. Natl. Acad. Sci. U. S. A.*, vol.

 doi:10.20944/preprints202102.0610.v1

106, no. 6, pp. 1942–1947, Feb. 2009.

[83] E. Irle, A. Barke, C. Lange, and M. Ruhleder, "Parietal abnormalities are related to avoidance in social anxiety disorder: A study using voxel-based morphometry and manual volumetry," *Psychiatry Res. - Neuroimaging*, vol. 224, no. 3, pp. 175–183, Dec. 2014.

[84] W. Liao *et al.*, "Selective aberrant functional connectivity of resting state networks in social anxiety disorder," *Neuroimage*, vol. 52, no. 4, pp. 1549–1558, Oct. 2010.

[85] C. Imperatori *et al.*, "Default mode network alterations in individuals with high-trait-anxiety: An EEG functional connectivity study," *J. Affect. Disord.*, vol. 246, pp. 611–618, 2019.

[86] S. Eldawlatly and K. Oweiss, "Graphical Models of Functional and Effective Neuronal Connectivity," in *Statistical Signal Processing for Neuroscience and Neurotechnology*, Elsevier Inc., 2010, pp. 129–174.